Photoinduced Perfluoroalkylation Mediated by Cobalt Complexes Supported by Naphthyridine Ligands

Photoinduced perfluoroalkylation mediated by cobalt complexes supported by naphthyridine ligands

Hoan Minh Dinh,[a] R. Govindarajan,[a] Shubham Deolka,[a] Robert R. Fayzullin,[b] Serhii Vasylevskyi,[a] Eugene Khaskin,[a] and Julia R. Khusnutdinova*

[a] Okinawa Institute of Science and Technology Graduate University, Coordination Chemistry and Catalysis Unit, 1919-1 Tancha, Onna-son, Okinawa 904-0495, Japan

[b] Arbuzov Institute of Organic and Physical Chemistry, FCR Kazan Scientific Center, Russian Academy of Sciences, 8 Arbuzov Street, Kazan 420088, Russian Federation

ABSTRACT: Cobalt(III) and cobalt(II) perfluoroethyl complexes supported by 1,8-naphthyridine or its mono- or dimethylsubstituted analogs were synthesized and their reactivity has been investigated in light-induced radical perfluoroethylation of arenes and heteroarenes. Similar to previously reported Ni^{III} complexes, Co^{III} naphthyridine-based complexes show light-induced Co^{III}–C_2F_5 bond homolysis to generate the C_2F_5 radical, while the Co^{II} complex was significantly less reactive. In the presence of a stoichiometric amount of electron-rich arene or heteroarene, the products of mono-perfluoroethylation by the cationic $[(naphthyridine)_2Co^{III}(C_2F_5)_2]^+$ complexes were obtained selectively and with good yields. This reactivity was further enhanced in the presence of one-electron oxidants or benzoquinone. Moderate catalytic turnover was obtained when pentafluoroethyl-1,2-benziodoxol-3(1*H*)-one (Acid C_2F_5-Togni reagent) was used, although the substrate scope and the reactivity remain limited to electron-rich substrates.

INTRODUCTION

Radical C–H trifluoromethylation catalyzed by base metal complexes attracts significant attention as a convenient synthetic tool to introduce fluorine atoms into organic compounds, which may be used to improve stability and alter the activity of biologically active compounds and pharmaceuticals.[1-8] While trifluoromethylation mediated by first-row transition metal complexes, especially Ni[9-11] and Cu,[12-23] recently became the subject of active research, using this methodology to introduce longer perfluoroalkyl chains is significantly less studied, although the presence of longer perfluoroalkyl groups may have a significant effect on pharmacokinetic properties of organic compounds as compared to trifluoromethyl group.[24-25] In 2021, the Vicic group described perfluoroalkylation by using solvated perfluoroalkyl nickel(II) complexes that also showed catalytic reactivity in trifluoromethylation. However, only stoichiometric reactivity was observed in perfluoroethylation.[11] Recently, our group reported a simple catalytic protocol for perfluoroalkylation of arenes and heteroarenes by using solvated nickel(II) bis(perfluoroalkyl) complexes in combination with commercially available Togni-type reagents containing perfluoroethyl or perfluoropropyl groups.[26]

While high valent Ni complexes have been actively studied in catalytic or stoichiometric C–H bond trifluoromethylation,[9-11] cobalt complexes received significantly less attention as they are generally considered to be less active as compared to nickel.[11] However, the reactivity of Co complexes may be tuned by supporting ligands. As an example, the Soper group achieved light-induced stoichiometric C(sp^2)–H bond trifluoromethylation mediated by a cobalt(III) trifluoromethyl complex supported by a redox-noninnocent [OCO] pincer ligand.[27] Vitamin B_{12} (cobalamin) derivative containing ester-derivatized tetradentate corrin macrocyclic ligand has been reported as a catalyst for combined electrochemical/photochemical perfluoroalkylation of electron-rich arenes via a light-induced radical formation,[28-29] resembling biologically relevant Co-C(sp^3) bond cleavage in coenzyme B_{12}-dependent enzymes.[30-33] Photolytic Co-C cleavage has also been reported to occur more easily for longer-chain cobaloxime(III) perfluoroalkyl complexes as compared to the Co-CF_3 analogs.[34]

Considering that our group has recently developed a visible-light-induced catalytic trifluoromethylation using Ni^{III} complexes supported by simple naphthyridine or dimethylnaphthyridine ligands,[35] we sought to expand this reactivity to Co using simple naphthyridine ligands. Since Co precursors with longer perfluoroalkyl chains are synthetically accessible, we focused on using perfluoroethyl Co complexes supported by naphthyridines to induce Co-C bond homolysis via light irradiation, and whether these complexes can be active in stoichiometric C(sp^2)–H bond perfluoroalkylation.

In this work, we synthesized a number of Co complexes with naphthyridine and perfluoroalkyl ligands and performed an in-depth examination of their structural and electronic properties. We demonstrate that these complexes undergo light-induced Co-perfluoroalkyl bond homolysis that does not require the presence of multidentate, redox-active or macrocyclic ligands and can be achieved in Co^{III} complexes supported by bidentate N-donor naphthyridine ligands. Preliminary studies showed that these complexes have the potential for catalytic C(sp^2)–H perfluoroethylation with the commercially available perfluoroethyl Togni reagent, albeit limited only to electron-rich substrates. The most active complex was an air-stable Co^{III} species, however, at this point, these complexes are relatively less active than the nickel complexes used in our group.

RESULTS AND DISCUSSION

Neutral cobalt complexes. Our first efforts to obtain naphthyridine Co^{III} complexes were focused on the use of a common $Co^{III}(MeCN)_3(C_2F_5)_3$ precursor reported by the Vicic group.[36] This precursor was conveniently obtained by the reaction of anhydrous $CoBr_2$ with 3 equiv. of AgF and 4 equiv. of TMS-C_2F_5. Treatment of $Co^{III}(MeCN)_3(C_2F_5)_3$ with 1 equiv. of 1,8-naphthyridine (**L1**) in tetrahydrofuran (THF) solution at room temperature (RT) for 16 hours led to the formation of a neutral complex Co(**L1**)(MeCN)$(C_2F_5)_3$ (**1**), which was isolated as a pale yellow solid obtained in 65 % yield (Scheme 1). The neutral complex **2** with a monomethyl-substituted 2-methyl-1,8-naphthyridine ligand (**L2**) was obtained in a similar way and isolated in 68 % yield. Complexes **1** and **2** were characterized by multinuclear NMR spectroscopy, electrospray ionization high-resolution mass-spectrometry (ESI-HRMS), UV-vis and FT-IR spectroscopy, elemental analysis, and single-crystal X-ray diffraction (SC-XRD). SC-XRD analysis reveals a distorted octahedral geometry around the *fac*-Co$(C_2F_5)_3$ fragment, supported by one κ^2-coordinated naphthyridine and one MeCN ligand (Figure 1, a-b).

The ^{1}H NMR spectrum of **1** exhibits a set of three multiplets in the aromatic region corresponding to the **L1** ligand and consistent with the presence of a plane of symmetry. The ^{19}F NMR spectrum exhibits two types of inequivalent C_2F_5 groups, characterized by two signals for CF_3 group in a 2 : 1 ratio at –80.58 and –80.79 ppm, respectively. Due to the presence of unsymmetrical ligand **L2**, complex **2** features 5 aromatic peaks of the **L2** ligand, while all three C_2F_5 groups are inequivalent in the ^{19}F NMR spectrum.

SC-XRD analysis reveals that for complexes **1** and **2** the Co–C lengths for C_2F_5 trans to N-atoms of naphthyridine are in a range of 1.942(3)-1.987(2) Å, while Co–C bond *trans* to MeCN is in the range of 1.976(6)-1.981(2) Å (Table 1).

Interestingly, introducing two methyl substituents in 2,7-dimethyl-1,8-naphthyridine (**L3**) led to the formation of two isomeric complexes when this ligand was treated with $Co^{III}(MeCN)_3(C_2F_5)_3$ (Scheme 1). When the reaction was followed by NMR spectroscopy in acetone-d_6, almost full consumption of **L3** was observed already after 1 hour at RT, along with the appearance of a major product **3a**, accompanied by a minor species **3b** with a ratio of **3a** : **3b** being 20 : 1. The aromatic peaks of the major product appear as two doublets at 8.53 and 7.71 ppm and one signal for the Me group, consistent with coordination to a *fac*-Co(C_2F_5) fragment. This was further confirmed by SC-XRD study of the yellow crystals obtained from pentane/THF solution from the reaction mixture at –30 °C (Figure 1, c). The minor species **3b** becomes the predominant product when the reaction mixture is further heated for 16 hours at 65 °C leading to the formation of a **3a** : **3b** mixture formed in a 1 : 4 ratio. Orange crystals obtained were analyzed by SC-XRD showing the isomeric structure **3b** with a *mer*-Co$(C_2F_5)_3$ configuration, with the MeCN ligand trans to an N-atom of **L3** (Figure 1, d). This is also consistent with the lack of a mirror plane evident from the ^{1}H NMR spectrum, showing four doublets at 8.51, 8.47, 7.74, and 7.53 ppm in the aromatic region and two singlets of the inequivalent Me groups of **L3** at 2.81 and 2.62 ppm.

Scheme 1. Synthesis of neutral pentafluoroethyl cobalt(III) complexes.

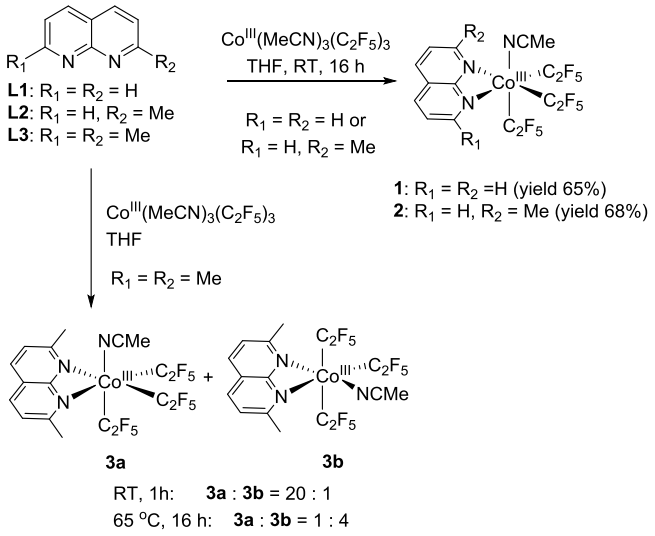

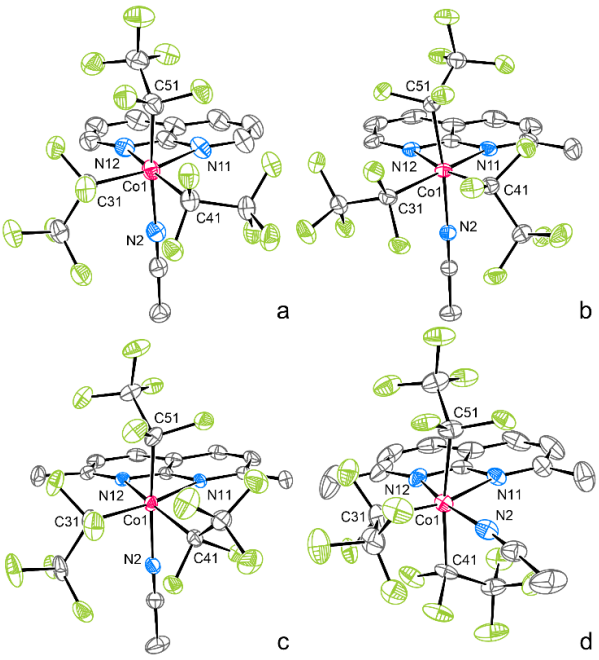

Figure 1. ORTEP of **1** (a), **2** (b), **3a** (c), and **3b** (d) at 50 % probability level according to single-crystal X-ray diffraction. Minor disorder components and hydrogen atoms are omitted for clarity.

Table 1. Selected internuclear distances [Å] for 1-3b according to single-crystal X-ray diffraction. Data for the main disorder component are present. Atomic numbering scheme is given in Figure 1.

Bond	**1**	**2**	**3a**	**3b**
Co1–N11	2.082(4)	2.130(2)	2.082(3)	2.045(5)
Co1–N12	2.057(4)	2.073(2)	2.123(3)	1.996(6)
Co1–N2	1.959(4)	1.9645(17)	1.974(3)	1.881(6)
Co1–C31	1.963(6)	1.987(2)	1.965(3)	1.933(13)
Co1–C41	1.982(5)	1.942(3)	1.987(4)	2.047(6)
Co1–C51	1.976(6)	1.981(2)	1.963(4)	2.085(15)

Further heating at 65 °C for 2 days did not lead to the exclusive formation of **3b** and the isomeric ratio remained unchanged,

indicating that isomers **3a** and **3b** have similar stability, with the kinetic product, *fac*-isomer **3a**, being slightly less thermodynamically favorable, likely due to the steric bulk imposed by two *ortho*-Me substituents located in proximity to C_2F_5 ligands as opposed to one MeCN ligand and one C_2F_5 group in the thermodynamic product, isomer *mer*-**3b**. This is also consistent with relative stability obtained by comparing DFT-optimized structures showing that **3b** is marginally more stable than **3a** by 0.26 kcal mol^{-1} (see SI).

As **3a** showed a set of broadened peaks in the ^{19}F NMR spectrum even at low temperature, the full assignment was done only for complex **3b** that features well-defined multiplets. ^{19}F COSY NMR analysis showed that the signal splitting pattern is mainly determined by the long-range coupling between apical (perpendicular to **L1** plane) and equatorial (in-plane with **L1**) C_2F_5 groups across the Co atom[36-37] as well as geminal coupling within the apical CF_2 groups, virtually in the absence of observed vicinal coupling. Near-zero or very small vicinal coupling constants are commonly observed in perfluoroalkylated compounds (and some perfluoroalkyl metal complexes),[36] which could arise from the averaging effect due to the internal rotations and cancellation of coupling constant contributions of opposite signs.[38-40] Thus, long-range coupling gives rise to the observed signal multiplicity. For example, the CF_3 groups of apical C_2F_5 ligands appear as a triplet due to coupling to the CF_2 group of equatorial C_2F_5, and the CF_3 group of equatorial C_2F_5 appears as a triplet of triplets due to coupling to two pairs of inequivalent fluorines of CF_2 groups of the apical C_2F_5.

Monocationic Co^{III} complexes. Considering that our previous study identified that cationic $[(\mathbf{L3})_2Ni^{III}(CF_3)_2]^+$ complexes supported by two naphthyridine-based ligands were active in light-induced trifluoromethylation,[35] we sought to obtain a similar structural motif in Co complexes requiring the presence of only two C_2F_5 groups and two naphthyridine ligands, as opposed to neutral complexes **1**-**3**. To obtain such complexes, a different synthetic approach was selected based on the formation of a bis(naphthyridine)$Co^{II}Cl_2$ precursor by the treatment of anhydrous $CoCl_2$ with 2 equiv. of **L1** or **L2** in MeOH-CH_2Cl_2 solution at RT for 16 hours (Scheme 2). Complexes **4** and **5** were isolated in 70 and 98% yields, respectively, and characterized by UV-vis, FT-IR spectroscopy, ESI-HRMS, elemental analysis, and SC-XRD. The alternative synthesis of complex **4** has also been reported in the literature by treatment of $CoCl_2 \cdot 6H_2O$ with naphthyridine in DMF/MeOH mixture and its crystal structure has also been confirmed by SC-XRD.[41] The SC-XRD analysis revealed a distorted tetrahedral Co center in **4** and **5** with naphthyridine ligands coordinated in a monodentate fashion (Figure 2, a-b and Table 2). The analogous reaction of $CoCl_2$ with 2 equiv. of **L3** also afforded complex **6** isolated in 64 % yield. In contrast to **4** and **5**, SC-XRD analysis shows a distorted octahedral structure around the cobalt center in complex **6**, with two **L3** ligands coordinating in a bidentate fashion (Figure 2, c). The magnetic moment measured by the Evans method for methanol-d_4 solutions of **4**, **5**, and **6** were 4.65, 5.06, and 4.88 μ_B, respectively, consistent with a high-spin d^7 configuration (S=3/2) for the Co^{II}.

Scheme 2. Synthesis of complexes 4-9.

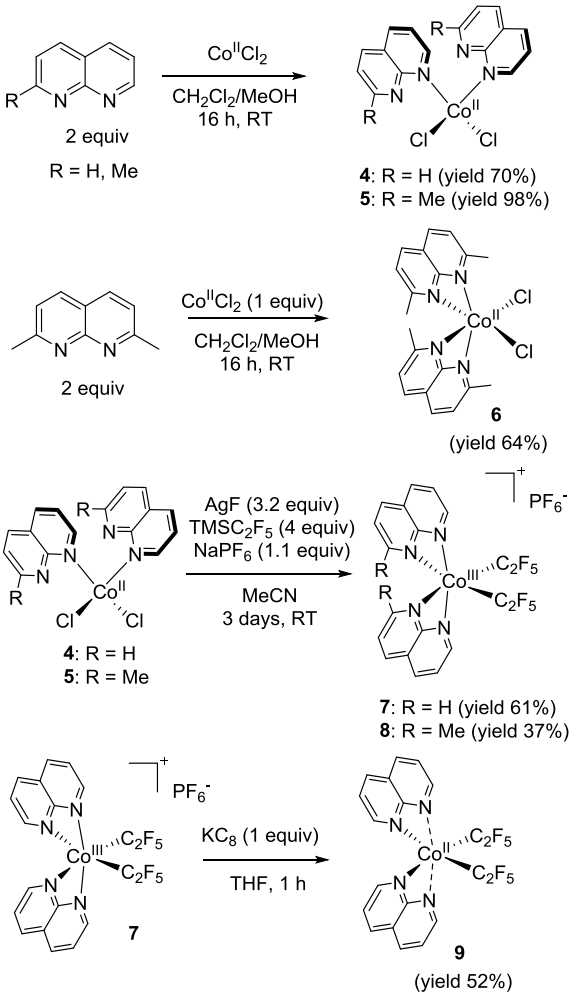

Table 2. Selected internuclear distances [Å] for 4-6 according to single-crystal X-ray diffraction. For 5, data for one of three symmetry-independent molecules are present. Atomic numbering scheme is given in Figure 2.

Bond	**4**	**5**	**6**
Co1–N11	2.0381(17)	2.0267(19)	2.272(2)
Co1–N12	3.0177(18)	2.738(2)	2.188(2)
Co1–N21	2.0371(16)	2.040(2)	2.269(2)
Co1–N22	3.0860(17)	2.9134(19)	2.183(2)
Co1–Cl1	2.2770(5)	2.2747(7)	2.3748(7)
Co1–Cl2	2.2679(5)	2.2867(7)	2.3512(7)

Table 3. Selected internuclear distances [Å] for 7-9 according to single-crystal X-ray diffraction. Atomic numbering scheme is given in Figure 2.

Bond	**7**	**8**	**9**
Co1–N11	2.074(5)	2.0778(17)	1.9918(16)
Co1–N12	1.926(4)	1.9429(17)	2.5049(18)
Co1–N21	2.073(5)	2.0765(16)	1.9954(17)
Co1–N22	1.942(4)	1.9354(16)	2.4053(17)
Co1–C31	1.948(6)	1.949(2)	1.9451(19)
Co1–C41	1.935(6)	1.9443(19)	1.957(2)

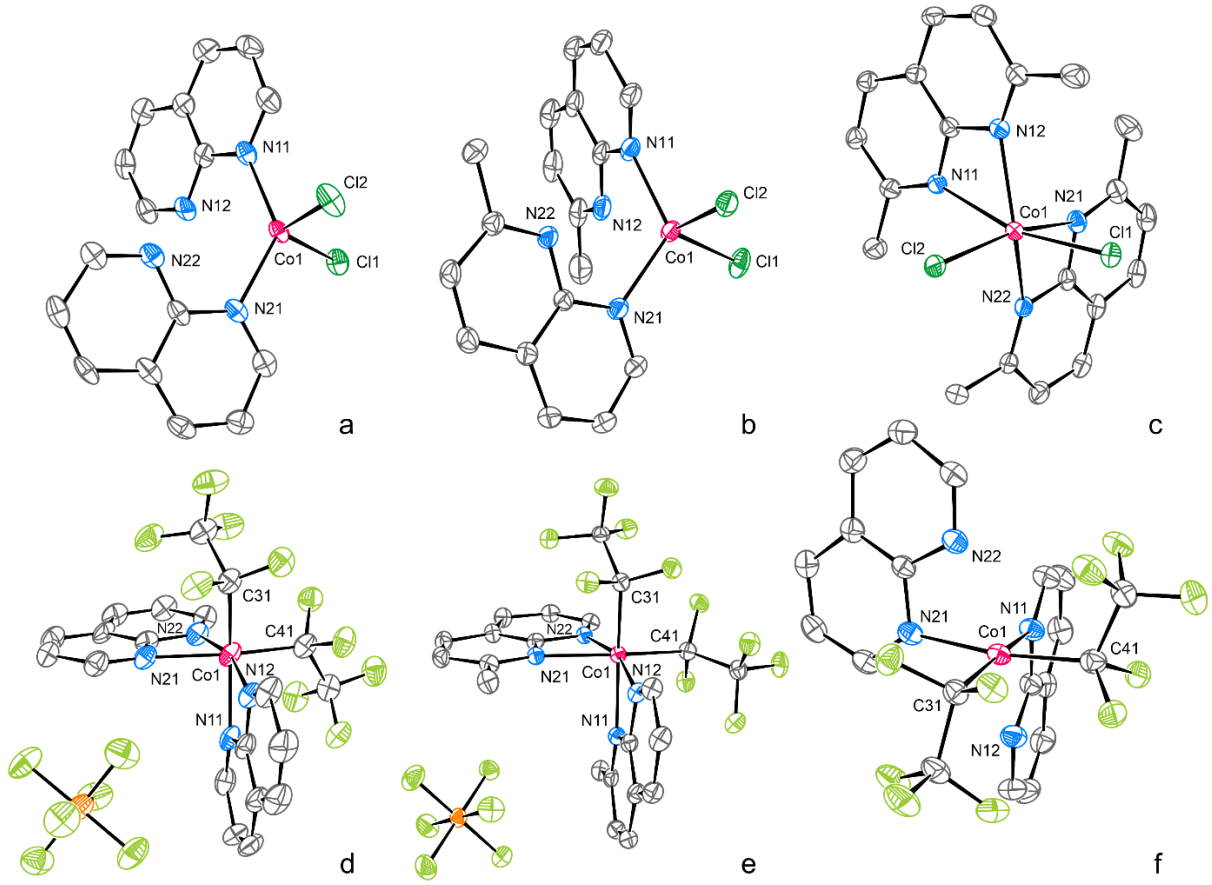

Figure 2. ORTEP of **4** (a), **5** (b), **6** (c), **7** (d), **8** (e), and **9** (f) at 80 % (**4**) or 50 % (**5**-**9**) probability level. Minor disorder components, solvent molecules, and hydrogen atoms are omitted for clarity. For **5**, one of three symmetry-independent molecules is shown

.

Further treatment of **4** with an excess amount of $Me_3SiC_2F_5$ in the presence of 3 equiv. of AgF and 1 equiv. of $NaPF_6$ in acetonitrile afforded Co^{III} complex **7** isolated in 61% yield as an orange crystalline solid (Scheme 2). Complex **7** was stable in air for months in solid form. Similarly, complex **8** was obtained in 37 % isolated yield by treatment of complex **5** with 3 equiv. of AgF, 3.5 equiv. Me_3Si-C_2F_5, and 1 equiv. of $NaPF_6$ in acetonitrile. Complexes **7** and **8** were characterized by multinuclear NMR, UV-vis, IR spectroscopy, ESI-HRMS, elemental analysis, and SC-XRD (Figure 2 and Table 3). The analogous reaction with complex **6** led to the formation of a mixture of two unidentified products that could not be isolated by crystallization or unambiguously characterized by other methods.

SC-XRD confirms that complex **7** contains a cationic Co^{III} center with two C_2F_5 groups present in *cis*-positions to each other and two naphthyridine ligands coordinating in a bidentate fashion (Figure 2, d). The equivalent C_2F_5 ligands are characterized by the presence of two doublets of unresolved multiplets for the geminally coupled F-atoms of the CF_2 group at –86.13 ppm and –94.08 ppm as well as one triplet at –81.58 ppm (J_{FF} ~ 5 Hz) corresponding to the CF_3 groups. The uncoordinated hexafluorophosphate counteranion appears at –72.81 ppm as a doublet. Similar structure (Figure 2, e) and NMR features were established for complex **8**, showing two doublets in ^{19}F NMR spectrum at –84.27 ppm and –94.08 ppm corresponding to the geminally coupled CF_2 and one unresolved multiplet at –81.77 ppm assigned to the CF_3 groups, as well as uncoordinated hexafluorophosphate counteranion.

Electrochemical properties and synthesis of a Co^{II} complex. The isolated series of cationic and neutral Co^{III} complexes were then investigated by cyclic voltammetry to gain insight into the accessibility of other oxidation states for Co–C_2F_5 species. The anodic scan revealed irreversible oxidation waves at high potentials (>1 V vs. Fc^+/Fc) for complexes **1**-**3**, while the cathodic scan shows at least two irreversible reduction processes at highly negative potentials (ca. -1.6 V vs Fc^+/Fc for the first wave), showing that both higher and lower oxidation states are not easily accessible and are unlikely to provide stable products (see Figure 3 and SI). In contrast, both cationic complexes **7** and **8** are characterized by the presence of a quasireversible reduction wave characterized by the cathodic peak potential of –0.76 V and –0.90 V vs. Fc^+/Fc, respectively, along with two additional reduction waves at significantly more negative potentials. This suggests that Co^{II} species may be easily accessible and provide stable products for bis-pentafluoroethyl Co complexes.

When complex **7** was subjected to a reduction in the presence of potassium graphite (KC_8) in THF, a deep-red solution was formed, from which a neutral Co^{II} complex **9** was isolated in 52 % yield. The magnetic moment measured by the Evans

method for an acetone-d_6 solution of **9** was 1.85 μ_B, suggesting an S=½ ground state corresponding to a low-spin d^7 configuration for the Co^{II} center.

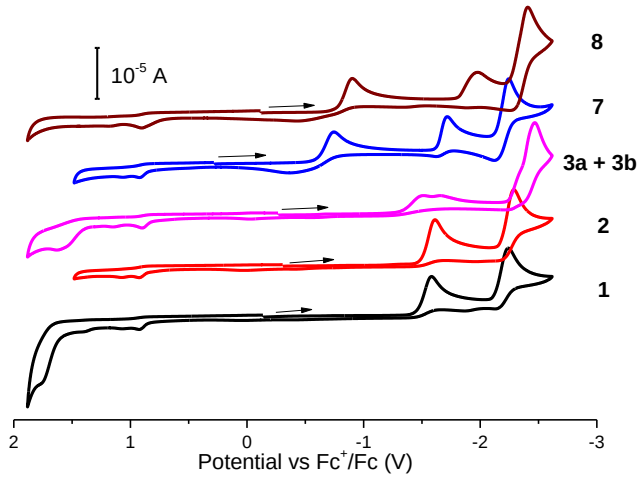

Figure 3. Cyclic voltammograms of complex **1**, **2**, **3a + 3b** (**3a : 3b** = 1 : 4), **7**, and **8** (2 mM) in 0.1 M $^nBu_4NClO_4$/MeCN solution at 23 °C (scan rate 100 mV s^{-1}; 1.6 mm glassy carbon disk working electrode; the arrow indicates the initial scan direction).

According to SC-XRD (Figure 2, e and Table 3), Co atom is bound to two C_2F_5 groups and two naphthyridine ligands, with short Co–N11 (1.9918(16) Å) and Co1–N21 (1.9954(17) Å) distances present *trans* to carbon atoms of C_2F_5, and significantly longer Co–N12 and Co–N22 distances, 2.5049(18) and 2.4053(17) Å, *cis* to C_2F_5 ligands. Such inequivalent distances and axially elongated octahedral structure could be attributed to the Jahn–Teller distortion; a similar elongated octahedral environment was observed in d^7 Ni^{III} complexes with **L3** ligand reported earlier.[35]

To further elucidate the bonding interactions in complex **9**, the DFT-optimized structure of **9** was analyzed using the quantum theory of atoms in molecules (QTAIM). According to computations, all interactions in the coordination sphere of atom Co1 in complex **9** are characterized by the small positive values of the electron density ρ_b and the Laplacian of electron density $\nabla^2\rho_b$ at the corresponding bond critical points (Figure 4 and Table 4), with the lower values of the electron density at the bond critical points located along axially elongated Co-N bonds (see SI for details).

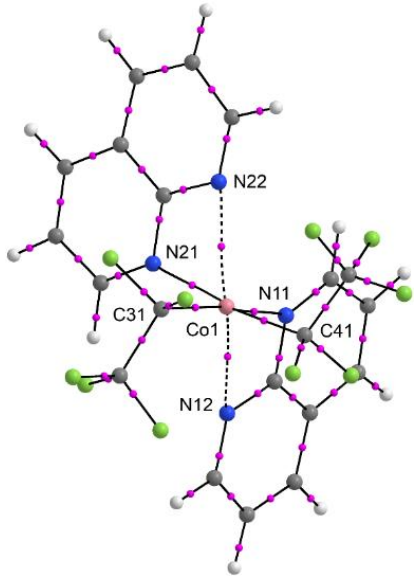

Figure 4. Molecular graph of gas-phase optimized complex **9**. Bond critical points and bond paths are shown as magenta spheres and black lines. These elements are omitted if the value of electron density at the bond critical point is less than 0.02 a.u. If the value of electron density at the bond critical point is less than 0.03 a.u., the corresponding bond paths are shown as dashed lines.

Table 4. Selected internuclear distances (d, Å) as well as the values of the electron density (ρ_b, a.u.), its Laplacian ($\nabla^2\rho_b$, a.u.), and delocalization indices at the corresponding critical bond points for gas-phase optimized complex 9.

Bond	d^a	$\rho_b{}^b$	$\nabla^2\rho_b{}^c$	DI^d
Co1–N11	2.03749	0.070901	0.430733	0.435116
Co1–N12	2.45412	0.029185	0.122357	0.192274
Co1–N21	2.03659	0.071073	0.431815	0.436411
Co1–N22	2.45659	0.029079	0.121303	0.190935
Co1–C31	1.97454	0.111561	0.294288	0.753186
Co1–C41	1.97537	0.111342	0.294331	0.752245

Photoinduced Co–C_2F_5 bond homolysis and C–H bond perfluoroethylation.

First, to assess the ability of the obtained complexes to undergo Co–C bond homolysis, the complexes were exposed to 14 W blue LED irradiation (465 nm) in the presence of 2 equiv. of 2,2,6,6-tetramethyl-1-piperidinyloxyl (TEMPO) as the radical trap (Table 5). Irradiation of neutral complexes **1**, **2** or an isomeric mixture containing complexes **3a** and **3b** (**3a** : **3b** = 1 : 4) with blue LED light for 1 hour at RT resulted in the formation of a TEMPO-C_2F_5 adduct, which was detected by ^{19}F NMR spectroscopy (Table 5).[26, 42] The yield was determined by ^{19}F NMR integration against α,α,α-trifluorotoluene as an internal standard showing moderate amounts of TEMPO-C_2F_5 ranging between 21 to 46% yield based on the amount of Co complex. Similarly, irradiation of cationic complexes **7** and **8** resulted in the formation of TEMPO-C_2F_5 adduct, with the highest yield obtained for naphthyridine-supported complex **7**. The exposure of complexes **7** or **8** to 2 equiv. of TEMPO in the absence of light did not produce any desired product. For comparison, ir-

radiation of a Co precursor, $Co^{III}(MeCN)_3(C_2F_5)_3$ in the presence of TEMPO under analogous conditions resulted in 18 % NMR yield of TEMPO-C_2F_5. These results suggest that similar to previously reported Ni^{III} complexes,[35] visible light irradiation of Co^{III} complexes induced the formation of a C_2F_5 radical trapped by TEMPO, and the reactivity is enhanced if naphthyridine ligand is present. Interestingly, irradiation of a Co^{II} complex **9** with blue LED under analogous conditions afforded only a small amount of TEMPO-C_2F_5 adduct suggesting that the light-induced bond homolysis is presumably less efficient for Co^{II} oxidation state.

While the Co-containing product could not be isolated in a pure form, ESI-MS analysis of the solution of **7** after irradiation with blue LED in the absence of TEMPO shows the presence of a peak characterized by *m/z* 438.0344, which was assigned to the cationic $[Co^{II}(\mathbf{L1})_2(C_2F_5)]^+$ fragment (calculated *m/z* 438.0309) resulting from the loss of one C_2F_5 group (Scheme 3). Similarly, irradiation of complex **8** and analysis of the reaction mixture by ESI-HRMS allowed us to detect the corresponding peak of $[Co^{II}(\mathbf{L2})_2(C_2F_5)]^+$ characterized by *m/z* 466.0659 (calculated *m/z* 466.0622).

Table 5. Photoinduced Co-C_2F_5 bond homolysis trapped by TEMPO.

Entry	Complex	Modification of standard conditions	Yield of TEMPO-C_2F_5 (%)[a]
1	**1**	None	21
2	**2**	None	46
3	**3a+3b**	None	46
4	**7**	None	74
5	**8**	None	37
6	**9**	None	6
7	$Co(C_2F_5)_3(MeCN)_3$	None	18
8	**7**	No blue LED	Not detected

[a]Yields were determined by ^{19}F NMR integration against α,α,α-trifluorotoluene as an internal standard.

Scheme 3. Photoinduced Co^{III}-C_2F_5 bond homolysis in complex 7.

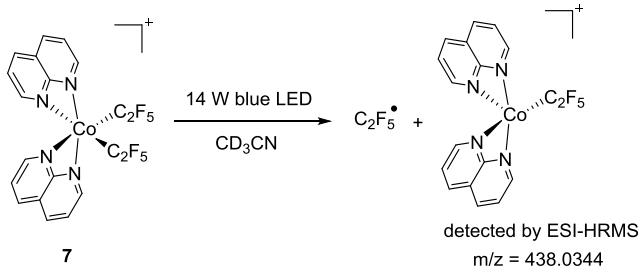

To evaluate the ability of Co^{III} complexes to perform arene perfluoroethylation under stoichiometric conditions, Co pentafluoroethyl complexes were irradiated with blue LED light in the presence of one equiv. of an electron-rich substrate, N-phenylpyrrole (**Ia**) or 1,3,5-trimethoxybenzene (**Ib**) for 24 hours at RT in acetonitrile-d_3 (Table 6). The highest yields of monoperfluoroethyl-substituted products **IIa** and **IIb** were obtained in the presence of cationic bis-naphthyridine-based complexes **7** and **8**, while much lower yields were observed in the presence of neutral complexes **1**-**3**. Co^{II} complex **9** and the precursor $Co^{III}(MeCN)_3(C_2F_5)_3$ produced only trace amounts of the pentafluoroethylated product in the case of N-phenylpyrrole, while 1,3,5-trimethoxybenzene produced no detectable amounts of perfluoroethylated products in the presence of **9**. In the absence of light, the reaction of **Ia** or **Ib** with complex **7** produced no pentafluoroethylated product.

Table 6. Stoichiometric C-H perfluoroethylation of Ia and Ib by cobalt complexes.[a]

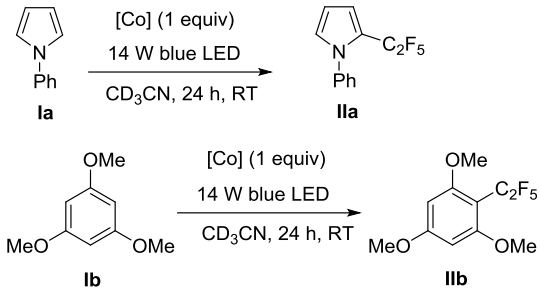

Entry	Substrate	[Co] complex	Product	Yield (%)[b]
1	**Ia**	**1**	**IIa**	24
2	**Ia**	**2**	**IIa**	29
3	**Ia**	**3a+3b**	**IIa**	54
4	**Ia**	**7**	**IIa**	60
5	**Ia**	**8**	**IIa**	59
6	**Ia**	**9**	**IIa**	2
7	**Ia**	**7**[c]	**IIa**	n.d.
8	**Ia**	$Co(MeCN)_3(C_2F_5)_3$	**IIa**	3
9	**Ib**	**1**	**IIb**	11
10	**Ib**	**2**	**IIb**	24
11	**Ib**	**3a+3b**	**IIb**	15
12	**Ib**	**7**	**IIb**	58
13	**Ib**	**8**	**IIb**	43
14	**Ib**	**9**	**IIb**	n.d.
15	**Ib**	**7**[c]	**IIb**	n.d.
16	**Ib**	$Co(MeCN)_3(C_2F_5)_3$	**IIb**	10

[a]The reactions were performed under N_2 atmosphere for 24 hours using 1 equiv. of substrate and 1 equiv. of a complex in acetonitrile-d_3 at RT under blue light LED (465 nm) unless indicated otherwise [b]Yields were determined by ^{19}F NMR integration against α,α,α-trifluorotoluene as an internal standard. [c]Without 14W blue LED irradiation. n.d. – not detected.

In all cases, only the mono-perfluoroethylation product was obtained and di-substituted products could not be detected in NMR and GC-MS analysis. C_2F_5H was found in all cases as a byproduct with the yield ranging from 3 to 15%, which was confirmed by ^{19}F NMR, while no other fluorine-containing side-products were detected.

Among naphthyridine-supported cobalt(III) complexes used in this study, complexes **7** and **8** show greater absorption in the visible region due to the presence of broad bands at 474 nm and 473 nm (Figure 5) showing better overlap with blue LED emission (465 nm), which also correlates with their greater photoinduced perfluoroalkylation reactivity. By contrast, complexes **1**-**3** show less efficient absorption in this range. At the same time, unreactive complex **9** shows a visible absorption band centered at 471 nm; however, its lack of reactivity could in part be due to the low stability of an expected Co^{I} product of Co^{II}–C bond homolysis due to poor stabilization of this low oxidation state by N-donor ligands.

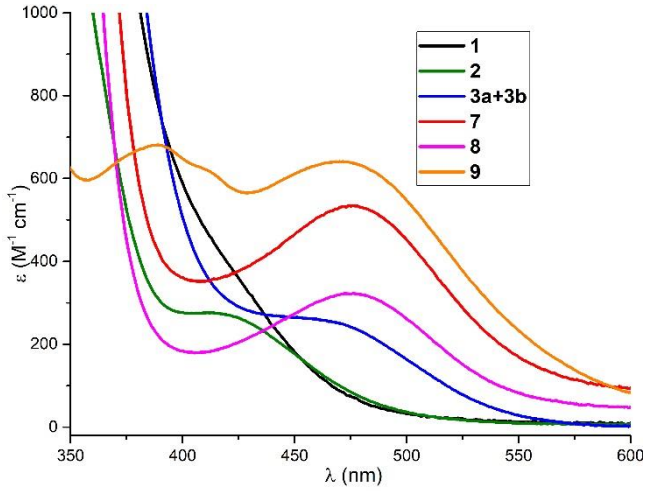

Figure 5. Overlay of UV-vis absorption spectra of complexes **1**, **2**, **3a** + **3b**, **7**, **8**, and **9** in MeCN.

To assess the reactivity with other substrates, complex **7** was reacted with arenes and heteroarenes under standard conditions (Scheme 4) resulting in the formation of perfluoroethyl derivatives in moderate or low yields in the case of 3-methylindole (72%) or mesitylene (33%) and showing no reactivity with electron-poor *meta*-dichlorobenzene.

Scheme 4. Reactivity of 7 with other substrates in stoichiometric perfluoroethylation.

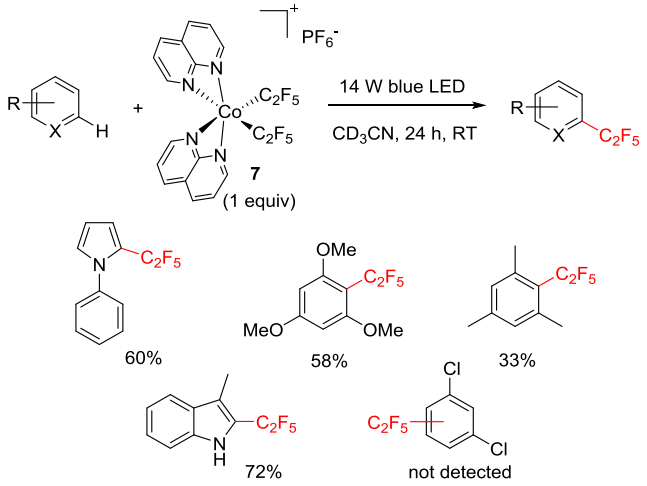

By analogy with the previous literature and consistent with radical trap experiments, the formation of a perfluoroethyl-substituted arene in a stoichiometric reaction likely involves the initial C_2F_5 radical formation via a light-induced Co^{III}-C bond homolysis, followed by the C_2F_5 radical attack at the electron-rich arene to give a radical adduct **III**. The proposed pathway is shown in Scheme 5 for the reaction mediated by cationic complexes **7** and **8**, although a similar mechanism could be operating in the case of neutral complexes **1**-**3**. Rearomatization of **III** via oxidation/deprotonation or a formal hydrogen atom loss would then produce a pentafluoroethyl-substituted arene. Considering that no sacrificial reagents were used in a stoichiometric perfluoroethylation, the starting material (complex **7** or **8**) could serve as a sacrificial oxidant to give inactive **9** and H^+. Alternatively, the light-induced C_2F_5 radical release could occur from product **IV** followed by H-atom abstraction from **III** to give C_2F_5H. This could limit the reaction yield to give only 58-60% of perfluoroethylated arene in the best cases reported in Table 5 along with the formation of small amount of C_2F_5H (ca. 5-7 % in the presence of **7**) during the reaction. To examine the effect of base and oxidant additives, we first performed perfluoroethylation of **Ia** in the presence of free naphthyridine ligand and 2,6-di-*tert*-butyl-pyridine, which could potentially trap the proton released during the reaction. However, slightly diminished yields were obtained (Table 7). Complex **7** was found to be moderately stable in the presence of 1 equiv. of HBF_4, with 68% complex remaining unreacted after 24 h at RT showing that a small amount of acid released during the reaction may be tolerated under these conditions.

On the other hand, the addition of one-electron oxidants, copper(II) triflate or ferrocenium, provided improved yields of perfluoroethylated product **IIa** (65-73%) compared to the control experiment under the same conditions (50-60%). Similarly, the improved yield was observed in the presence of 1,4-benzoquinone, which can serve as an acceptor of both protons and electrons. On the other hand, azobenzene had a detrimental effect, presumably due to its significant absorption in the visible region and competing reactivity. Considering that higher oxidation states are not accessible for **7** using these mild oxidants, one of the possible explanations for the limited yield in stoichiometric perfluoroethylation by **7** is its role as a sacrificial reagent via reduction to inactive **9** by **III** in the absence of external oxidants, or unproductive release of C_2F_5H via an H-atom abstraction by the C_2F_5 radical.

Scheme 5. Proposed pathway for perfluoroethylated arene formation in the presence of cationic complexes 7 or 8.

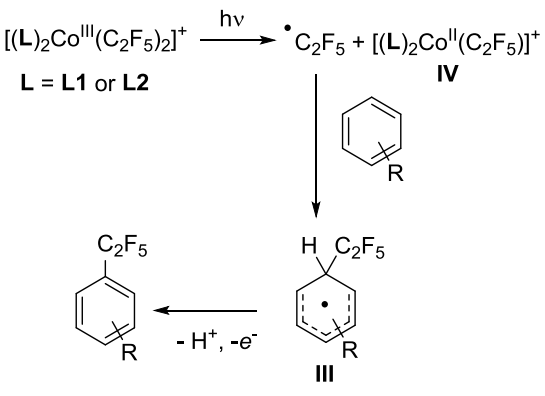

Table 7. Stoichiometric C-H pentafluoroethylation of Ia mediated by 7 with the presence of additives.

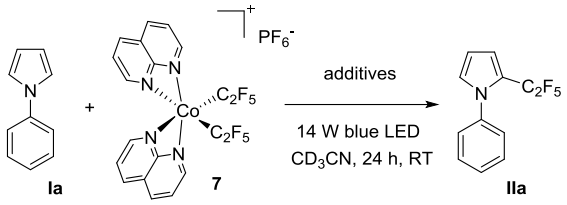

Entry	Additive	Equiv.	Yield of **IIa** (%)
1	1,8-naphthyridine	2	44
2	2,6-ditertbutylpyridine	2	41
3	$Cu(OTf)_2$	1	73
4	$Fc^+PF_6^-$	1	65
5	benzoquinone	1	70
6	azobenzene	1	43
7	none		50

One notable feature of the stoichiometric mono-perfluoroethylation of electron-rich arenes by **7** and **8** is the formation of the product in moderate yields even in the presence of only one equiv. of a substrate relative to a complex, while the majority of such radical trifluoromethylation protocols report using a large excess of a substrate, likely to avoid side reactions such as double perfluoroalkylation. This prompted us to look into the possibility of developing catalytic perfluoroethylation in the presence of **7**.

Ni-catalyzed trifluoromethylation is often performed using Umemoto reagent or trifluoromethanesulfonyl chloride, pentafluoro-analogs of these reagents are not easily accessible and for many impractical to use due to cost, and our initial attempts to regenerate **7** using TMS-C_2F_5 and oxidant failed to give catalytic results. We continued to investigate catalytic reactivity with other C_2F_5 sources and found that the pentafluoroethyl-1,2-benziodoxol-3(1*H*)-one (Acid C_2F_5-Togni reagent, **V**) a commercially available pentafluoroethylation source (Table 8) which was previously utilized for Ni-catalyzed perfluoroalkylation gave catalytic activity with Co.

The model substrate 1-phenylpyrrole was treated with Acid C_2F_5-Togni reagent **V** in the presence of 10 mol% of complex **7** under blue LED light, which produced selectively mono-perfluoroethylated product in 76 % yield after 24 h at RT in DMSO-d_6 or CD_3CN as a solvent. In the absence of complex **7**, a notably lower yield was obtained (32%), while the reaction in the absence of LED light produced only 14% of product **IIa**.

Table 8. Perfluoroethylation of Ia using Acid C_2F_5-Togni reagent IV and complex 7.

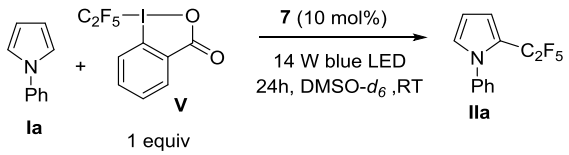

Entry	Modification of standard conditions	Yield (%)
1	None	76
2	CD_3CN instead of DMSO-d_6	76
3	No catalyst **7** present	32
4	No blue LED irradiation	14

Using these conditions, other arene and heteroarene substrates were tested showing that only electron-rich N-phenylpyrrole and 1,3,5-trimethoxybenzene showed appreciable reactivity, while mesitylene and *meta*-dichlorobenzene were mostly unreacted, and attempted perfluoroethylation of 3-methylindole produced the product in low yields (Scheme 6). Although catalytic turnover is possible under these conditions using catalyst **7**, the results are overall less competitive compared to Ni-catalyzed perfluoroalkylation.[26] We will further investigate the possibility of using other approaches to the regeneration of Co perfluoroalkyl species to enable catalytic perfluoroalkylation of arenes.

Scheme 6. Scope of pentafluoroethylation catalyzed by 7.

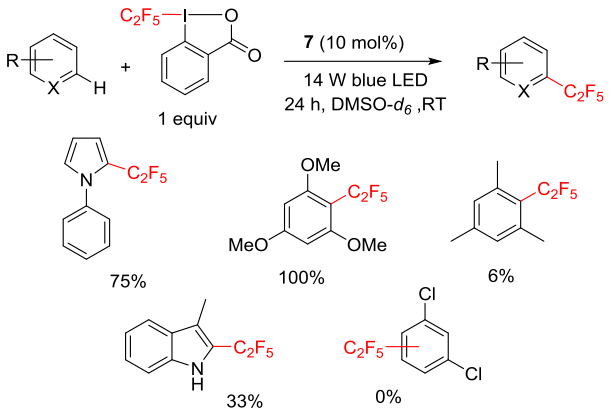

SUMMARY AND CONCLUSIONS

In this work, the reactivity of a new family of Co^{III} and Co^{II} perfluoroethyl complexes supported by 1,8-naphthyridine ligand or its mono- and dimethylsubstituted analogs was tested in light-induced bond homolysis and arene or heteroarene perfluoroethylation. Stoichiometric photoinduced perfluoroethylation of $C(sp^2)$-H bonds was observed only for Co^{III} complexes, while Co^{II} complexes were generally unreactive. Selective, stoichiometric mono-perfluoroethylation that does not require excess (hetero)arene substrate or redox-noninnocent ligands was observed, showing that simple naphthyridine ligands promote this reactivity, with best results obtained for cationic complexes **7** and **8**. Although initial results indicate the possibility of catalytic turnover with Togni-type reagent, the substrate scope remains limited to electron-rich substrates and the reactivity is generally less competitive compared to the reported nickel catalysts. We will direct some attempts toward developing methods for the regeneration of catalytically competent Co^{III}-perfluoroalkyl complexes using inexpensive sources of perfluoroalkyl groups (e.g., TMS-C_2F_5, perfluoroalkyl iodides or via transmetalation).

The ultimate aim of this research direction in our group is to develop sustainable and economically viable methods for selective arene and heteroarene functionalization and to introduce perfluoroalkyl chains other than the commonly used trifluoromethyl group. Considering that our group developed some of the main methods for this with the much more active nickel complexes however, including a ligand-free method, this study can be seen as an important addendum that explores the possible

role of cobalt catalysts in such reaction. Ultimately, a number of interesting Co perfluoroalkyl complexes with simple naphthyridine were synthesized and their oxidation and redox properties were explored. The air stability of most of the species may lead to possible applications in other, non-catalytic areas.

EXPERIMENTAL SECTION

General specifications: All reactions were performed using standard Schlenk or glovebox techniques under a dry nitrogen atmosphere if not indicated otherwise. Unless noted otherwise, all chemicals were purchased from major commercial suppliers (TCI, Sigma-Aldrich, and Nacalai-Tesque) and used without purification. Anhydrous solvents were dispensed from an MBRAUN solvent purification system and degassed prior to use. Anhydrous deuterated solvents were purchased from Eurisotop and stored over 4 Å molecular sieves. $Co(MeCN)_3(C_2F_5)_3$ were prepared according to the literature procedure[36]. NMR spectra were recorded on a JEOL ECS400S 400 MHz and JEOL ECZ600R 600 MHz. The following abbreviations are used for describing NMR spectra: s (singlet), d (doublet), t (triplet), m (multiplet), dd (doublet of doublets), tt (triplet of triplets), tq (triplet of quartets), vd (virtual doublet), br (broad). A typical Evans method magnetic moment measurement was done in a coaxial tube containing the solvent and the internal standard. Electrospray ionization high-resolution mass spectrometry (ESI-HRMS) measurements were performed on a Thermo Scientific ETD apparatus using MeOH or MeCN as a solvent for injection. Elemental analyses were performed using an Exeter Analytical CE440 instrument. Solid-state FT-IR spectra were recorded using an Agilent Cary 630 with an ATR module in an argon-filled glovebox. The following abbreviations are used for describing FT-IR spectra: s (strong), m (medium), w (weak), and br (broad). UV-vis spectra were recorded on an Agilent Cary 60 spectrophotometer. The X-ray diffraction data for single crystals **1-9** were recorded on a Rigaku Xtalab Pro diffractometer or a Bruker D8 Venture diffractometer. Cyclic voltammetry experiments were performed on an ALS CHI 660E electrochemical workstation under N_2 atmosphere. Electrochemical grade tetrabutylammonium perchlorate (TBAP) from Sigma-Aldrich was used as the supporting electrolyte in anhydrous MeCN as a solvent. A glassy carbon disk electrode (d = 1.6 mm) was used as a working electrode. A non-aqueous Ag-wire reference electrode assembly was filled with 0.01M $AgNO_3$ in 0.1 M TBAP/MeCN solution as a reference electrode. A Pt-wire was used as an auxiliary electrode. The reference electrode was calibrated against $FeCp_2$ (Fc), where the Fc/Fc^+ couple vs $Ag/AgNO_3$/MeCN. Blue LED light was purchased from Akiba LED, 14W, 465 nm.

Synthesis of 1: In a glove box, 50.0 mg (0.384 mmol) of 1,8-naphthyridine and 207.1 mg (0.384 mmol, 1 equiv.) of *fac*-$(MeCN)_3Co(C_2F_5)_3$ were dissolved in 5 mL of THF. The reaction mixture was stirred at room temperature for 16 hours. The yellow resulting solution was then crystallized by slow diffusion of pentane to yield **1** as yellow crystals. Yield: 146 mg (65%). ^{1}H NMR (600 MHz, –30 °C, acetone-d_6): δ 9.09 (vd, J_{HH} = 4.9 Hz, o-$\boldsymbol{H}_{Naph}$, 2H), 8.86 (dd, J_{HH} = 8.4, 1.6 Hz, p-$\boldsymbol{H}_{Naph}$, 2H), 8.03 (dd, J_{HH} = 8.4, 4.8 Hz, m-$\boldsymbol{H}_{Naph}$, 2H), 2.14 (s, C$\boldsymbol{H}_3$-CN, 3H). ^{19}F NMR (565 MHz, –30 °C, acetone-d_6) δ -80.58 (br s, C$\boldsymbol{F}_3$-CF_2, 6F), -80.79 (br s, CF_3-C$\boldsymbol{F}_2$, 3F), -94.88 - -96.67 (m, CF_3-C$\boldsymbol{F}_2$, 4F). ^{13}C{^{1}H} NMR (151 MHz, –30 °C, acetone-d_6) δ 159.42 (quat.-$\boldsymbol{C}_{Naph}$), 156.03 (o-$\boldsymbol{C}_{Naph}$), 139.80 (p-$\boldsymbol{C}_{Naph}$), 126.33 (m-$\boldsymbol{C}_{Naph}$), 125.45 (C$\boldsymbol{F}_3$-CF_2), 123.15, 121.35 (quat.-$\boldsymbol{C}_{Naph}$), 121.23, 119.31, 117.39 2.44 (C$\boldsymbol{H}_3$-CN). The carbon atom of the nitrile group could not be identified due to low intensity. Peaks at 123.15, 121.23, 119.31, and 117.39 ppm were not clearly identified due to splitting from F and low intensity. ESI-HRMS (*m/z*): found (calcd.): $C_{14}H_9Co_1F_{10}N_3^+$: 467.9897 (467.9963). Elemental analysis found (calcd.): $C_{16}H_9Co_1F_{15}N_3$: C 33.20 (32.73), H 1.53 (1.54), 6.96 (7.16). UV-Vis (CH_3CN), λ, nm (ε, M^{-1} cm^{-1}): 425 (360), 357 (1880), 308 (9430). FT-IR (ATR, solid): 3163 (br), 2999 (br), 2944 (br), 2291 (m), 2252 (s), 1434 (m), 1418 (br), 1374 (s), 1038 (s), 747 (s), 665 (m), 654 (m).

Synthesis of 2: In a glove box, 27.0 mg (0.188 mmol) of 2-methyl-1,8-naphthyridine and 101.1 mg (0.188 mmol, 1 equiv.) of *fac*-$(MeCN)_3Co(C_2F_5)_3$ were dissolved in 3 mL of THF. The reaction mixture was stirred at room temperature for 16 hours. The yellow resulting solution was then crystallized by slow diffusion of pentane to yield **2** as yellow crystals. Yield: 76.5 mg (68%). ^{1}H NMR (600 MHz, –30 °C , acetone-d_6): δ 9.13 (d, $^3J_{HH}$ = 5.2 Hz, o-$\boldsymbol{H}_{Naph}$, 1H), 8.80 (d, $^3J_{HH}$ = 8.2 Hz, p-$\boldsymbol{H}_{Naph}$, 1H), 8.68 (d, $^3J_{HH}$ = 8.5 Hz, p-$\boldsymbol{H}_{Naph}$, 1H), 7.97 (dd, J_{HH} = 8.3, 5.0 Hz, m-$\boldsymbol{H}_{Naph}$, 1H), 7.83 (d, $^3J_{HH}$ = 8.4 Hz, m-$\boldsymbol{H}_{Naph}$, 1H), 2.76 (s, $\boldsymbol{H}_{Me}$, 3H), 2.23 (s, C$\boldsymbol{H}_3$CN, 3H). ^{19}F NMR (565 MHz, –30 °C , acetone-d_6) δ -78.86 (br s, C$\boldsymbol{F}_3$-CF_2, 3F), -79.89 (br s, C$\boldsymbol{F}_3$-CF_2, 3F), -81.01 (d, $^2J_{FF}$ = 256.8 Hz, CF_3-C$\boldsymbol{F}_2$, 1F), -81.09 (br s, C$\boldsymbol{F}_3$-CF_2, 3F), -88.26 (d, $^2J_{FF}$ = 237.9 Hz, CF_3-C$\boldsymbol{F}_2$, 1F), -91.83 (d, $^2J_{FF}$ = 258.9 Hz, CF_3-C$\boldsymbol{F}_2$, 1F), -97.36 (d, $^2J_{FF}$ = 238.1 Hz, CF_3-C$\boldsymbol{F}_2$, 1F), -98.45 (d, $^2J_{FF}$ = 259.2 Hz, CF_3-C$\boldsymbol{F}_2$, 1F), -100.39 (d, $^2J_{FF}$ = 259.0 Hz, CF_3-C$\boldsymbol{F}_2$, 1F). ^{13}C{^{1}H} NMR (151 MHz, –30 °C, acetone-d_6) δ 210.13 (CH_3-$\boldsymbol{C}$N), 168.66 (quat.-$\boldsymbol{C}_{Naph}$), 159.63 (quat.-$\boldsymbol{C}_{Naph}$), 155.20 (o-$\boldsymbol{C}_{Naph}$), 139.62 (p-$\boldsymbol{C}_{Naph}$), 138.99 (p-$\boldsymbol{C}_{Naph}$), 128.62 (m-$\boldsymbol{C}_{Naph}$), 126.09 (C$\boldsymbol{F}_3$-CF_2), 125.14 (m-$\boldsymbol{C}_{Naph}$), 119.81 (quat.-$\boldsymbol{C}_{Naph}$), 22.91 ($\boldsymbol{C}_{Me}$), 2.53 (C$\boldsymbol{H}_3$-CN). The carbon atoms of C_2F_5 could not be identified due to splitting from F and low intensity. ESI-HRMS (*m/z*): found (calcd): $C_{15}H_{11}Co_1F_{10}N_3^+$: 482.0055 (482.0120). Elemental analysis found (calcd): $C_{17}H_{11}Co_1F_{15}N_3$: 34.15 (33.96), 1.61 (1.84), 7.03 (6.91). UV-Vis (CH_3CN), λ, nm (ε, M^{-1} cm^{-1}): 425 (260), 311 (9097), 267 (9867). FT-IR (ATR, solid): cm^{-1} 3162 (br), 3002 (br), 2943 (br), 2292 (m), 2251 (s), 1441 (s), 1428 (m), 1374 (s), 1038 (s), 917 (s), 747 (s).

Synthesis of 3a + 3b: In a glove box, 31.6 mg (0.2 mmol) of 2,7-bis(methyl)-1,8-naphthyridine (**L3**) and 107.8 mg (0.2 mmol, 1 equiv.) of *fac*-$(MeCN)_3Co(C_2F_5)_3$ were dissolved in 5 mL of THF. The mixture was then transferred to a 25 mL Schlenk flask and brought out of the glove box. The reaction was heated at 65 °C for 16 hours to yield a mixture **3a : 3b** = 1 : 4 . The resulting orange solution was then crystallized by slow diffusion of pentane to yield **3a : 3b** = 1 : 4 as orange crystals. Yield: 76.5 mg (68%). ESI-HRMS (*m/z*): found (calcd): $C_{16}H_{13}Co_1F_{10}N_3^+$: 496.0214 (496.0274). EA found (cald): $C_{18}H_{13}Co_1F_{15}N_3$: C 35.14 (35.14), H 1.71 (2.13), N 6.72 (6.83). UV-Vis (CH_3CN), λ, nm (ε, M^{-1} cm^{-1}): 450 (265), 311 (16142). FT-IR (ATR, solid, cm^{-1}): 3163 (br), 3003 (br), 2943 (br), 2291 (s), 2251 (s), 1779 (br), 1694 (br), 1440 (s), 1429 (br), 1374 (s), 1037 (s), 917 (s), 748 (s), 674 (s). ^{1}H NMR for **3a** (600 MHz, 23 ºC, acetone-d_6): δ 8.53 (d, $^3J_{HH}$ = 8.3 Hz, $\boldsymbol{H}_{naph}$, 2H), 7.71 (d, $^3J_{HH}$ = 8.3 Hz, $\boldsymbol{H}_{naph}$, 2H), 2.79 (s, C$\boldsymbol{H}_3$, 6H). ^{1}H NMR for **3b** (600 MHz, 23 ºC, acetone-d_6): δ 8.51 (d, $^3J_{HH}$ = 8.5 Hz, $\boldsymbol{H}_{naph}$, 1H), 8.47 (d, $^3J_{HH}$ = 8.4 Hz, $\boldsymbol{H}_{naph}$, 1H), 7.74 (d, $^3J_{HH}$ = 8.5 Hz, $\boldsymbol{H}_{naph}$, 1H), 7.53 (d, $^3J_{HH}$ = 8.4 Hz, 1H), 2.81 (s, C$\boldsymbol{H}_3$, 3H), 2.65 (s, C$\boldsymbol{H}_3$-CN, 3H), 2.62 (s, C$\boldsymbol{H}_3$, 3H). ^{19}F peaks of **3a** are broadened in the ^{19}F NMR spectrum and could not be fully resolved even at low temperature. In the ^{19}F NMR spectrum obtained for **3a : 3b** = 1 :4 mixture, only peaks of **3b** could be clearly assigned (eq = equatorial C_2F_5 in-plane with naphthyridine; ap – apical C_2F_5 groups perpendicular to naphthyridine place): ^{19}F NMR of **3b** (565 MHz, 23 ºC, acetone-d_6): δ -75.68 (br m, CF_3-C$\boldsymbol{F}_2$ eq, 2F), -79.24 (tt, $^5J_{FF}$ = 9.2, 25 Hz, C$\boldsymbol{F}_3$-CF_2 eq, 3F), -81.75 (t, $^3J_{FF}$ = 7.8 Hz, C$\boldsymbol{F}_3$-CF_2 ap, 6F), -96.82 (dq, $^2J_{FF}$ = 283 Hz, $^5J_{FF}$ = 8.5 Hz,CF_3-C$\boldsymbol{F}$F ap, 2F), -103.11 (doublet of multiplets, $^2J_{FF}$ = 284 Hz, CF_3-CF$\boldsymbol{F}$ ap, 2F). ^{13}C{^{1}H} NMR of **3a : 3b** = 1 : 4 (151 MHz, 23 ºC, acetone-d_6) δ 210.03, 170.44, 168.24, 167.40, 159.27, 138.79, 138.69, 138.04, 133.43, 129.14, 127.97, 127.83, 127.51, 124.44, 124.23, 124.01, 122.52, 122.31, 122.10, 120.79, 120.57, 120.39, 118.86, 118.64, 118.15, 116.29, 69.20, 68.04, 66.10, 54.95, 54.78, 54.66, 54.53, 22.25, 22.20, 22.15, 21.42.

Observation of the 3a+3b (**3a** : **3b** = 20 : 1) **formation at RT:** In a glove box, 2.9 mg (0.18 mmol) of **L3** and 10.0 mg (0.18 mmol, 1 equiv.) of *fac*-$(MeCN)_3Co(C_2F_5)_3$ were dissolved in 1 mL of acetone-d_6. The reaction mixture was stirred at room temperature for 1 hour, and then was analyzed by ^{1}H NMR, showing the formation of a mixture **3a : 3b** = 20 : 1. Single crystals of **3a** could be obtained by diffusing pentane to the solution at –30 °C.

Synthesis of 4: 200.0 mg of **L1** (1.537 mmol, 2 equiv.) and 41.0 mg of $CoCl_2$ (0.768 mmol, 1 equiv.) were dissolved in 10 mL of 2:1 DCM-MeOH mixture. The dark blue solution was then stirred vigorously at room temperature for 16 h, then recrystallized by diffusing ether to the mother solution to yield **4** as blue crystals. Yield: 210 mg (70%). EA found (calcd) : $C_{16}H_{12}Co_1Cl_2N_4$: C 48.45 (49.26), H 2.84 (3.10), N 13.89 (14.36). ESI-HRMS (*m/z*): found (calcd): $C_{16}H_{12}Co_1Cl_1N_4^+$: 354.0080 (354.0077). UV-Vis (CH_3OH), λ, nm (ε, M^{-1} cm^{-1}): 530 (11), 301 (15024). FT-IR (ATR, solid): 3047 (br), 1595 (s), 1498 (s), 1391

(m), 1293 (m), 1235 (m), 1197 (m), 1143 (s), 1128 (s), 1062 (s), 1034 (m), 956 (m), 841 (s), 800 (s). 782 (s). μ_{eff} = 4.65 μB (298 K, Evans method, methanol-d_4).

Synthesis of 5: 200.0 mg of **L2** (1.387 mmol, 2 equiv.) and 89.6 mg of $CoCl_2$ (0.694 mmol, 1 equiv.) were dissolved in 15 mL of 2:1 DCM-MeOH mixture. The dark blue solution was then stirred vigorously at room temperature for 16 h and recrystallized by diffusing ether to the mother solution to yield **5** as blue crystals. Yield: 284.2 mg (98%). ESI-HRMS (*m/z*): found (calcd): $C_{18}H_{16}Co_1Cl_1N_4^+$: 382.0386 (382.0390). EA found (calcd) : $C_{18}H_{16}Co_1Cl_2N_4$: C 51.23 (51.70), H 3.75 (3.86), N 12.78 (13.40). UV-Vis (CH_3OH), λ, nm (ε, M^{-1} cm^{-1}): 315 (7535), 298 (8472), 7262 (257), 224 (7484). FT-IR (ATR, solid): 3048 (br), 1613 (s), 1566 (s), 1493 (s), 1421 (m), 1376 (s), 1300 (s), 1286 (s), 1218 (m), 1138 (s), 1132 (m), 1063 (m), 1035 (m), 909 (m), 847 (s), 798 (s), 708 (m), 656 (s). μ_{eff} = 5.06 μB (298 K, Evans method, methanol-d_4).

Synthesis **of 6:** 100.0 mg of **L3** (0.632 mmol, 2 equiv.) and 41.0 mg of $CoCl_2$ (0.316 mmol, 1 equiv.) were dissolved in 10 mL of 2:1 DCM-MeOH mixture. The dark blue solution was then stirred vigorously at room temperature for 16 h, then recrystallized by diffusing ether to the mother solution to yield **6** as blue crystals. Yield: 90 mg (64%). ESI-HRMS (*m/z*) found (calcd): $C_{20}H_{20}Co_1Cl_1N_4$+: 410.0692 (410.0703). UV-Vis (CH_3OH), λ, nm (ε, M^{-1} cm^{-1}): 316 (18660), 310 (15600), 253 (6900). 217 (27000). FT-IR (ATR, solid): 3061 (br), 3007 (br), 1609 (s), 1566 (m), 1509 (s), 1439 (s), 1377 (s), 1313 (s), 1252 (s), 1215 (m), 1141 (s), 1035 (m), 998 (m), 853 (s), 800 (s), 789 (br). μ_{eff} = 4.88 μB (298 K, Evans method, methanol-d_4).

Synthesis of 7: In a glovebox, 100.0 mg of AgF (0.820 mmol, 3.2 equiv.) and 180 μL of $TMSC_2F_5$ (1.03 mmol, 4 equiv.) were mixed in 10 mL of acetonitrile. The reaction mixture was stirred in a dark for 2 hours, then the mixture was transferred to a 20-mL vial containing 100.0 mg of **4** (0.256 mmol, 1 equiv.) and 47.4 mg of $NaPF_6$ (0.282 mmol, 1.1 equiv.). The mixture was stirred vigorously in the dark for 3 days. The resulting yellow-brown slurry was filtered over celite, and the solvent was removed under vacuum to yield an orange-red precipitate, which was washed by pentane. Orange single crystals were grown by slow diffusion of pentane to the THF solution of **6**. Yield: 109 mg (61%). ^{1}H NMR (400 MHz, 23 ºC, CD_3CN) δ 8.80 (dd, $^3J_{HH}$ = 8.5, 1.4 Hz, ***H***$_{Naph}$, 2H), 8.77 (dd, J_{HH} = 5.2, 1.4 Hz, ***H***$_{Naph}$, 2H), 8.73 (dd, J_{HH} = 8.6, 1.5 Hz, ***H***$_{Naph}$, 2H), 8.68 (dd, J_{HH} = 4.8, 1.5 Hz, ***H***$_{Naph}$, 2H), 7.90 (dd, J_{HH} = 8.5, 5.2 Hz, ***H***$_{Naph}$, 2H), 7.82 (dd, $^3J_{HH}$ = 8.5, 4.8 Hz, ***H***$_{Naph}$, 2H). ^{19}F NMR (564 MHz, 23 ºC, CD_3CN): δ -72.81 (d, $^1J_{PF}$ = 706.4 Hz, P***F***$_6$, 6 H), -81.58 (t, J_{FF} ~ 5 Hz, C***F***$_3$-CF_2, 6H), -86.13 (vd, $^2J_{FF}$ = 228.5 Hz, CF_3-C***F***$_2$, 2H), -94.08 (vd, $^2J_{FF}$ = 227.5 Hz, CF_3-C***F***$_2$, 2H). ^{13}C{^{1}H} NMR (101 MHz, 23 ºC, CD_3CN): δ 159.11 (quat.-***C***$_{Naph}$), 158.76 (*o*-***C***$_{,Naph}$), 155.53 (*p*-***C***$_{Naph}$), 141.69 (*o*-***C***$_{Naph}$), 140.60 (*p*-***C***$_{Naph}$), 127.60 (*m*-***C***$_{Naph}$), 127.43 (*o*-***C***$_{Naph}$), 121.43 (quat.-C_{Naph}). The carbon atoms of C_2F_5 could not be identified due to splitting from F and low intensity. ESI-HRMS (*m/z*): found (calcd): $C_{20}H_{12}Co_1F_{10}N_4^+$: 557.0245 (557.0229). EA found (calculated) $C_{20}H_{12}Co_1F_{16}N_4P_1$: C 33.81 (34.21), H 1.33 (1.72), N 7.93 (7.98). UV-Vis (CH_3CN), λ, nm (ε, M^{-1} cm^{-1}): 474 (534), 302 (22000). FT-IR (ATR, solid) 3162 (br), 3002 (br), 2943 (br), 2626 (br), 2405 (br), 2291 (s), 2251 (s), 1738 (m), 1442 (m), 1420 (br), 1374 (s), 1038 (s), 918 (s), 748 (s), 667 (m).

Synthesis of 8: In a glovebox, 97.1 mg of AgF (0.765 mmol, 3.2 equiv.) and 168 μL of $TMSC_2F_5$ (0.96 mmol, 4 equiv.) were mixed in 10 mL of acetonitrile. The reaction mixture was stirred in a dark for 2 hours, then the mixture was transferred to a 20-mL vial containing 100.0 mg of **5** (0.239 mmol, 1 equiv.) and 44.1 mg of $NaPF_6$ (0.263 mmol, 1.1 equiv.). The mixture was stirred vigorously in the dark for 3 days. The resulting yellow-brown slurry was filtered over celite, and the solvent was removed under vacuum to yield an orange-red precipitate, which was washed by pentane. Orange single crystals can be recrystallized by slow diffusion of pentane to the THF solution. Yield 64.2 mg (37%). ^{1}H NMR (400 MHz, 23 ºC, CD_3CN) δ 8.80 (d, $^3J_{HH}$ = 5.1 Hz, o-***H***$_{Naph}$, 2H), 8.75 (dd, J_{HH} = 8.3, 1.2 Hz, p-***H***$_{Naph}$, 2H), 8.54 (d, $^3J_{HH}$ = 8.7 Hz, p-***H***$_{Naph}$, 2H), 7.85 (dd, J_{HH} = 8.5, 5.1 Hz, m-***H***$_{Naph}$, 2H), 7.64 (d, $^3J_{HH}$ = 8.7 Hz, m-***H***$_{Naph}$, 2H), 1.77 (s, C***H***$_3$, 6H). ^{19}F NMR (564 MHz, 23 ºC, CD_3CN) δ -72.78 (d, $^1J_{PF}$ = 706.3 Hz, P***F***$_6$, 6F), -81.77 (m, CF_3-C***F***$_2$, 6H), -84.27 (vd, $^2J_{FF}$ = 226.2 Hz, CF_3-C***F***$_2$, 2F), -93.13 (vd, $^2J_{FF}$ = 219.8 Hz, CF_3-C***F***$_2$, 2F). ^{13}C{^{1}H} NMR (101 MHz, 23 ºC, CD_3CN): δ 168.25 (quat.-***C***$_{Naph}$), 159.19 (quat.-***C***$_{Naph}$), 157.95 (o-***C***$_{Naph}$), 141.74 (p-***C***$_{Naph}$), 139.54 (p-***C***$_{Naph}$), 129.49 (m-***C***$_{Naph}$), 126.72 (m-***C***$_{Naph}$), 119.24 (quat.-***C***$_{Naph}$), 21.42 (***C***$_{Me}$). The carbon atoms of C_2F_5 could not be identified due to splitting from F and low intensity. ESI-HRMS (*m/z*): found (calcd): $C_{22}H_{16}Co_1F_{10}N_4^+$: 585.0559 (585.0542). EA found (cald): 36.77 (36.18), 1.99 (2.21), 7.08 (7.67). UV-Vis (CH_3CN), λ, nm (ε, M^{-1} cm^{-1}): 473 (322), 304 (17130). FT-IR (ATR, solid): cm^{-1} 3162 (br), 3001 (br), 2943 (br), 2628 (br), 2405 (br), 2291 (s), 2251 (s), 1738 (m), 1442 (m), 1417 (br), 1374 (s), 1217 (br), 1038 (s), 917 (s), 747 (s), 667 (br).

Synthesis of 9: In a glove box, 100.0 mg (0.142 mmol) of complex **7** was dissolved in 5 mL of THF. The orange solution was then transferred to a 20-mL vial containing 19.3 mg (0.142 mmol, 1 equiv.) of potassium graphite and the reaction mixture was stirred for 3 hours. The mixture was filtered through celite to remove any precipitate, and the solvent was removed under a vacuum to yield a red-wine powder, which was washed with a copious amount of pentane. Red wine single crystals were recrystallized by slow diffusion of pentane to the THF solution of **9**. Yield: 41 mg (52%). μ_{eff} = 1.85 μB (298 K, Evans method, acetone-d_6). ESI-HRMS (*m/z*): found (calcd): $C_{18}H_{12}Co_1F_5N_4^+$: 438.0335 (438.0309). EA found (cald): $C_{20}H_{12}Co_1F_{10}N_4$: C 41.17 (43.11), H 1.85 (2.17), N 9.55 (10.05). UV-Vis (MeCN), λ, nm (ε, M^{-1} cm^{-1}): 471 (641), 389 (681), 296 (13250). FT-IR (ATR, solid) : 2972 (m), 2857 (m), 1459 (br), 1176 (br), 1067 (s), 907 (s).

Radical trap by TEMPO experiments: In a glove box, a specified cobalt complex (0.01 mmol) and 3.1 mg of TEMPO (0.02 mmol, 2 equiv.) were dissolved in 0.7 mL of acetonitrile-d_3. To the solution, 1.2 μL of α,α,α-trifluorotoluene (0.01 mmol, 1 equiv.) was added as an internal standard. The resulting solution was then transferred to a young NMR tube and was placed 2-3 cm far away from a 14 W blue LED light equipped with a fan. The reaction was irradiated under the blue LED for one hour. The yield of the reaction was determined by ^{19}F NMR integration against α,α,α-trifluorotoluene as an internal standard.

ESI-HRMS analysis of the reaction mixture containing cobalt(III) complexes after irradiation: In a glove box, 0.01 mmol of a Co^{III} complex (**7** or **8**) was dissolved in 1 mL of acetonitrile. The resulting solution was transferred to a J. Young NMR tube, which was then placed 2-3 cm far away from 14 W blue LED light equipped with a fan and irradiated for 30 minutes. The reaction mixture was immediately analyzed by ESI-HRMS. The HRMS analysis shows the appearance of a new peak, which was not present in the solution of the starting complexes before irradiation.

After irradiation of complex **7**, a new peak is assigned to $[Co(\mathbf{L1})_2(C_2F_5)]^+$ ($C_{18}H_{12}Co_1F_5N_4$): *m/z* observed (cald): 438.0344 (438.0309).

After irradiation of complex **8**, a new peak is assigned to $[Co(\mathbf{L2})_2(C_2F_5)]^+$ ($C_{20}H_{16}Co_1F_5N_4$): *m/z* observed (cald): 466.0659 (466.0622).

General procedure for stoichiometric C-H perfluoroethylation: In a glove box, an arene or heteroarene substrate (0.01 mmol) and cobalt complex (0.01 mmol, 1 equiv.) were dissolved in 1 mL of acetonitrile-d_3. The solution was transferred to a J. Young NMR tube, which was then placed 2-3 cm far away from a 14 W blue LED light and irradiated for 24 hours. The reaction setup was equipped with a fan to avoid heating from irradiation. After the completion of the reaction, α,α,α-trifluorotoluene (0.01 mmol, 1 equiv.) was added to the reaction mixture. The yields were determined by ^{19}F NMR integration against α,α,α-trifluorotoluene as an internal standard. The formation of C_2F_5H is established by NMR spectroscopy by comparison with literature reports[43-44] and the yields are shown for individual reaction mixtures in the Supporting Information.

A similar procedure was used for perfluoroethylation of N-phenylpyrrole in the presence of additives.

General procedure for perfluoroethylation in the presence of catalytic amount of 7 and Acid C_2F_5-Togni reagent: In a glove box, an arene or heteroarene substrate (0.05 mmol), complex **7** (3.5 mg, 0.005 mmol, 10 mol%) and 1-pentafluoroethyl-1,2-benziodoxol-3(1*H*)-one (18.3 mg, 0.05 mmol, 1 equiv.) were dissolved in 1 mL of DMSO-d_6 or different solvent. The mixture was then transferred to an 11 mL screw-cap reaction tube and sealed with electric tape to avoid gas exchange. The tube was placed 2-3 cm far away from a 14 W blue LED light and irradiated for 24 hours. The reaction setup was equipped

with a fan to avoid heating from irradiation. After the completion of the reaction, 6.1 μL of α,α,α -trifluorotoluene (0.01 mmol, 1 equiv.) were added to the reaction mixture as internal standard and the resulting mixture was analyzed by NMR and GS-MS spectroscopy. The yields were determined by ^{19}F NMR integration against α,α,α-trifluorotoluene as an internal standard.

Computational details. All DFT calculations were implemented in the Gaussian 16 program.[45] Geometries were optimized without symmetry restrictions using M06L functional[46] and SDD[47] (for Co)/6-31++g(d,p)[48-51] (for other elements) basis set; ground state corresponded to the absence of imaginary frequencies. For comparison of relative stabilities of **3a** and **3b**, the structures were optimized taking into account the solvent (acetone) effect via the SMD model.[52] The quantum-topological analysis of the calculated electron density for "gas-phase" and solution (acetone) optimized structures was performed within the quantum topological theory of atoms in molecules by means of the AIMAll package (v 19.10.12).[53]

ASSOCIATED CONTENT

Supporting Information

The Supporting Information is available free of charge via the Internet at http://pubs.acs.org.
Experimental details and characterization data (PDF)
Cartesian coordinates for DFT-optimized structures (XYZ)

Accession codes

CCDC 2234108-2234115 and 2236993-2236994 contains the supplementary crystallographic data for this paper. These data can be obtained free of charge via https://www.ccdc.cam.ac.uk/structures/.

AUTHOR INFORMATION

*E-mail for J.R.K.: juliak@oist.jp

ORCID:

Hoan Dinh: 0000-0003-3635-8533

R. Govindarajan: 0000-0002-4336-1936

Shubham Deolka: 0000-0002-0050-0780

Robert R. Fayzullin: 0000-0002-3740-9833

Serhii Vasylevskyi: 0000-0001-6219-6051

Eugene Khaskin: 0000-0003-1790-704X

Julia R. Khusnutdinova: 0000-0002-5911-4382

Notes

The authors declare no competing financial interests.

ACKNOWLEDGMENT

The authors thank the Instrumental Analysis section and Engineering section for technical support, the HPC facility for access to computational resources and OIST for funding. R. R. F. performed crystal structure determination within the assignment for the Kazan Scientific Center of RAS. The authors thank Tatiana Gridneva for assistance with computational analysis.

REFERENCES

1. Purser, S.; Moore, P. R.; Swallow, S.; Gouverneur, V. Fluorine in medicinal chemistry. *Chem. Soc. Rev.* **2008,** *37*, 320-330.
2. Hagmann, W. K. The Many Roles for Fluorine in Medicinal Chemistry. *J. Med. Chem.* **2008,** *51*, 4359-4369.
3. Müller, K.; Faeh, C.; Diederich, F. Fluorine in Pharmaceuticals: Looking Beyond Intuition. *Science* **2007,** *317*, 1881-1886.
4. Nagib, D. A.; MacMillan, D. W. C. Trifluoromethylation of arenes and heteroarenes by means of photoredox catalysis. *Nature* **2011,** *480*, 224-228.
5. Ji, Y.; Brueckl, T.; Baxter, R. D.; Fujiwara, Y.; Seiple, I. B.; Su, S.; Blackmond, D. G.; Baran, P. S. Innate C-H trifluoromethylation of heterocycles. *PNAS* **2011,** *108*, 14411-14415.
6. O'Brien, A. G.; Maruyama, A.; Inokuma, Y.; Fujita, M.; Baran, P. S.; Blackmond, D. G. Radical C-H Functionalization of Heteroarenes under Electrochemical Control. *Angew. Chem. Int. Ed.* **2014,** *53*, 11868-11871.
7. Sladojevich, F.; McNeill, E.; Börgel, J.; Zheng, S.-L.; Ritter, T. Condensed-Phase, Halogen-Bonded CF_3I and C_2F_5I Adducts for Perfluoroalkylation Reactions. *Angew. Chem. Int. Ed.* **2015,** *54*, 3712-3716.
8. Cui, L.; Matusaki, Y.; Tada, N.; Miura, T.; Uno, B.; Itoh, A. Metal-Free Direct C-H Perfluoroalkylation of Arenes and Heteroarenes Using a Photoredox Organocatalyst. *Adv. Synth. Catal.* **2013,** *355*, 2203-2207.
9. D'Accriscio, F.; Borja, P.; Saffon-Merceron, N.; Fustier-Boutignon, M.; Mézailles, N.; Nebra, N. C−H Bond Trifluoromethylation of Arenes Enabled by a Robust, High-Valent Nickel(IV) Complex. *Angew. Chem. Int. Ed.* **2017,** *56*, 12898-12902.
10. Meucci, E. A.; Nguyen, S. N.; Camasso, N. M.; Chong, E.; Ariafard, A.; Canty, A. J.; Sanford, M. S. Nickel(IV)-Catalyzed C–H Trifluoromethylation of (Hetero)arenes. *J. Am. Chem. Soc.* **2019,** *141*, 12872-12879.
11. Shreiber, S. T.; Vicic, D. A. Solvated Nickel Complexes as Stoichiometric and Catalytic Perfluoroalkylation Agents**. *Angew. Chem. Int. Ed.* **2021,** *60*, 18162-18167.
12. Mudarra, Á. L.; Martínez de Salinas, S.; Pérez-Temprano, M. H. Nucleophilic Trifluoromethylation Reactions Involving Copper(I) Species: From Organometallic Insights to Scope. *Synthesis* **2019,** *51*, 2809-2820.
13. Paeth, M.; Tyndall, S. B.; Chen, L.-Y.; Hong, J.-C.; Carson, W. P.; Liu, X.; Sun, X.; Liu, J.; Yang, K.; Hale, E. M.; Tierney, D. L.; Liu, B.; Cao, Z.; Cheng, M.-J.; Goddard, W. A., III; Liu, W. Csp^3–Csp^3 Bond-Forming Reductive Elimination from Well-Defined Copper(III) Complexes. *J. Am. Chem. Soc.* **2019,** *141*, 3153-3159.
14. Liu, S.; Liu, H.; Liu, S.; Lu, Z.; Lu, C.; Leng, X.; Lan, Y.; Shen, Q. C(sp^3)-CF_3 Reductive Elimination from a Five-Coordinate Neutral Copper(III) Complex. *J. Am. Chem. Soc.* **2020,** *142*, 9785-9791.
15. Tan, X.; Liu, Z.; Shen, H.; Zhang, P.; Zhang, Z.; Li, C. Silver-Catalyzed Decarboxylative Trifluoromethylation of Aliphatic Carboxylic Acids. *J. Am. Chem. Soc.* **2017,** *139*, 12430-12433.
16. Weske, S.; Schoop, R.; Koszinowski, K. The Role of Ate Complexes in the Copper-Mediated Trifluoromethylation of Alkynes. *Chem. Eur. J.* **2016,** *22*, 11310-11316.
17. Lu, Z.; Liu, H.; Liu, S.; Leng, X.; Lan, Y.; Shen, Q. A Key Intermediate in Copper-Mediated Arene Trifluoromethylation, [^{n}Bu$_4$N][Cu(Ar)(CF_3)$_3$]: Synthesis, Characterization, and C(sp^2)−CF_3 Reductive Elimination. *Angew. Chem. Int. Ed.* **2019,** *58*, 8510-8514.
18. Senecal, T. D.; Parsons, A. T.; Buchwald, S. L. Room Temperature Aryl Trifluoromethylation via Copper-Mediated Oxidative Cross-Coupling. *J. Org. Chem.* **2011,** *76*, 1174-1176.
19. Zhang, H.-R.; Feng, C.-C.; Chen, N.; Zhang, S.-L. Direct Arene Trifluoromethylation Enabled by a High-Valent Cu^{III}–CF_3 Compound. *Angew. Chem. Int. Ed.* **2022,** *61*, e202209029.
20. Dubinina, G. G.; Furutachi, H.; Vicic, D. A. Active Trifluoromethylating Agents from Well-Defined Copper(I)−CF_3 Complexes. *J. Am. Chem. Soc.* **2008,** *130*, 8600-8601.
21. Liu, H.; Wu, J.; Jin, Y.; Leng, X.; Shen, Q. Mechanistic Insight into Copper-Mediated Trifluoromethylation of Aryl Halides: The Role of CuI. *J. Am. Chem. Soc.* **2021,** *143*, 14367-14378.
22. Ye, Y.; Sanford, M. S. Merging Visible-Light Photocatalysis and Transition-Metal Catalysis in the Copper-Catalyzed Trifluoromethylation of Boronic Acids with CF_3I. *J. Am. Chem. Soc.* **2012,** *134*, 9034-9037.
23. Baya, M.; Joven-Sancho, D.; Alonso, P. J.; Orduna, J.; Menjón, B. M−C Bond Homolysis in Coinage-Metal [M(CF_3)$_4$]$^-$ Derivatives. *Angew. Chem. Int. Ed.* **2019,** *58*, 9954-9958.
24. Prchalová, E.; Štěpánek, O.; Smrček, S.; Kotora, M. Medicinal applications of perfluoroalkylated chain-containing compounds. *Future Med. Chem.* **2014,** *6*, 1201-1229.

25. Fujiwara, T.; O'Hagan, D. Successful fluorine-containing herbicide agrochemicals. *J. Fluorine Chem.* **2014,** *167*, 16-29.

26. Deolka, S.; Govindarajan, R.; Vasylevskyi, S.; Roy, M. C.; Khusnutdinova, J. R.; Khaskin, E. Ligand-free nickel catalyzed perfluoroalkylation of arenes and heteroarenes. *Chem. Sci.* **2022,** *13*, 12971-12979.

27. Harris, C. F.; Kuehner, C. S.; Bacsa, J.; Soper, J. D. Photoinduced Cobalt(III)−Trifluoromethyl Bond Activation Enables Arene C−H Trifluoromethylation. *Angew. Chem. Int. Ed.* **2018,** *57*, 1311-1315.

28. Hossain, M. J.; Ono, T.; Wakiya, K.; Hisaeda, Y. A vitamin B12 derivative catalyzed electrochemical trifluoromethylation and perfluoroalkylation of arenes and heteroarenes in organic media. *Chem. Commun.* **2017,** *53*, 10878-10881.

29. Ono, T.; Wakiya, K.; Hossain, M. J.; Shimakoshi, H.; Hisaeda, Y. Synthesis of Trifluoromethylated B12 Derivative and Photolysis of Cobalt(III)–Trifluoromethyl Bond. *Chem. Lett.* **2018,** *47*, 979-981.

30. Abeles, R. H.; Dolphin, D. The vitamin B12 coenzyme. *Acc. Chem. Res.* **1976,** *9*, 114-120.

31. Neil, E.; Marsh, G. Coenzyme B12 (cobalamin)-dependent enzymes. *Essays Biochem.* **1999,** *34*, 139-154.

32. Jensen, K. P.; Ryde, U. How the Co−C Bond Is Cleaved in Coenzyme B12 Enzymes: A Theoretical Study. *J. Am. Chem. Soc.* **2005,** *127*, 9117-9128.

33. Blaauw, R.; L. van der Baan, J.; Balt, S.; W. G. de Bolster, M.; W. Klumpp, G.; Kooijman, H.; L. Spek, A. Synthesis, structure and Co–C bond homolysis of an intramolecularly bridged (tetrahydrofurfuryl)cobalt(salen) complex: a simple model of enzyme-bound coenzyme B12. *Chem. Commun.* **1998**, 1295-1296.

34. Liebing, P.; Oehler, F.; Wagner, M.; Tripet, P. F.; Togni, A. Perfluoroalkyl Cobaloximes: Preparation Using Hypervalent Iodine Reagents, Molecular Structures, Thermal and Photochemical Reactivity. *Organometallics* **2018,** *37*, 570-583.

35. Deolka, S.; Govindarajan, R.; Khaskin, E.; Fayzullin, R. R.; Roy, M. C.; Khusnutdinova, J. R. Photoinduced Trifluoromethylation of Arenes and Heteroarenes Catalyzed by High-Valent Nickel Complexes. *Angew. Chem. Int. Ed.* **2021,** *60*, 24620-24629.

36. Shreiber, S. T.; Scudder, J. J.; Vicic, D. A. $[(MeCN)_3Co(C_2F_5)_3]$: A Versatile Precursor to Cobalt(III) Perfluoroethyl Complexes. *Organometallics* **2019,** *38*, 3169-3173.

37. Visser, H. D.; Oliver, J. P. Long-range across metal ^1H-^1H coupling in organometallic derivatives. *J. Magn. Reson.* **1970,** *3*, 117-121.

38. Hirao, K.; Nakatsuji, H.; Kato, H.; Yonezawa, T. Theoretical study of the fluorine-fluorine nuclear spin coupling constants. I. Importance of orbital and spin dipolar terms. *J. Am. Chem. Soc.* **1972,** *94*, 4078-4087.

39. Saika, A.; Gutowsky, H. S. AN UNUSUAL FLUORINE MAGNETIC RESONANCE MULTIPLET. *J. Am. Chem. Soc.* **1956,** *78*, 4818-4819.

40. Harris, R. K.; Woodman, C. M. NMR spectra of molecules containing CF_2 groups: Part 2. Perfluorbutane. *J. Mol. Spectrosc.* **1968,** *26*, 432-443.

41. Huang, X.-C.; Xu, R.; Chen, Y.-Z.; Zhang, Y.-Q.; Shao, D. Two Four-Coordinate and Seven-Coordinate CoII Complexes Based on the Bidentate Ligand 1, 8-Naphthyridine Showing Slow Magnetic Relaxation Behavior. *Chem. Asian J.* **2020,** *15*, 279-286.

42. Xu, J.; Qiao, L.; Ying, B.; Zhu, X.; Shen, C.; Zhang, P. Transition-metal-free direct perfluoroalkylation of quinoline amides at C5 position through radical cross-coupling under mild conditions. *Org. Chem. Front.* **2017,** *4*, 1116-1120.

43. Elleman, D. D.; Brown, L. C.; Williams, D. The nuclear magnetic resonance spectra of fluorocarbons: Part I. Halogenated ethanes. *J. Mol. Spectrosc.* **1961,** *7*, 307-321.

44. Foris, A. ^{19}F and ^1H NMR spectra of halocarbons. *Magn. Reson. Chem.* **2004,** *42*, 534-555.

45. Frisch, M. J.; Trucks, G. W.; Schlegel, H. B.; Scuseria, G. E.; Robb, M. A.; Cheeseman, J. R.; Scalmani, G.; Barone, V.; Petersson, G. A.; Nakatsuji, H.; Li, X.; Caricato, M.; Marenich, A. V.; Bloino, J.; Janesko, B. G.; Gomperts, R.; Mennucci, B.; Hratchian, H. P.; Ortiz, J. V.; Izmaylov, A. F.; Sonnenberg, J. L.; Williams; Ding, F.; Lipparini, F.; Egidi, F.; Goings, J.; Peng, B.; Petrone, A.; Henderson, T.; Ranasinghe, D.; Zakrzewski, V. G.; Gao, J.; Rega, N.; Zheng, G.; Liang, W.; Hada, M.; Ehara, M.; Toyota, K.; Fukuda, R.; Hasegawa, J.; Ishida, M.; Nakajima, T.; Honda, Y.; Kitao, O.; Nakai, H.; Vreven, T.; Throssell, K.; Montgomery Jr., J. A.; Peralta, J. E.; Ogliaro, F.; Bearpark, M. J.; Heyd, J. J.; Brothers, E. N.; Kudin, K. N.; Staroverov, V. N.; Keith, T. A.; Kobayashi, R.; Normand, J.; Raghavachari, K.; Rendell, A. P.; Burant, J. C.; Iyengar, S. S.; Tomasi, J.; Cossi, M.; Millam, J. M.; Klene, M.; Adamo, C.; Cammi, R.; Ochterski, J. W.; Martin, R. L.; Morokuma, K.; Farkas, O.; Foresman, J. B.; Fox, D. J. *Gaussian 16 Rev. C.01*, Wallingford, CT, 2016.

46. Zhao, Y.; Truhlar, D. G. A new local density functional for main-group thermochemistry, transition metal bonding, thermochemical kinetics, and noncovalent interactions. *J. Chem. Phys.* **2006,** *125*, 194101.

47. Andrae, D.; Häußermann, U.; Dolg, M.; Stoll, H.; Preuß, H. Energy-adjustedab initio pseudopotentials for the second and third row transition elements. *Theor. Chim. Acta* **1990,** *77*, 123-141.

48. Francl, M. M.; Pietro, W. J.; Hehre, W. J.; Binkley, J. S.; Gordon, M. S.; DeFrees, D. J.; Pople, J. A. Self‐consistent molecular orbital methods. XXIII. A polarization‐type basis set for second‐row elements. *J. Chem. Phys.* **1982,** *77*, 3654-3665.

49. Hariharan, P. C.; Pople, J. A. Accuracy of AH n equilibrium geometries by single determinant molecular orbital theory. *Mol. Phys.* **1974,** *27*, 209-214.

50. Hariharan, P. C.; Pople, J. A. The influence of polarization functions on molecular orbital hydrogenation energies. *Theor. Chim. Acta* **1973,** *28*, 213-222.

51. Hehre, W. J.; Ditchfield, R.; Pople, J. A. Self—Consistent Molecular Orbital Methods. XII. Further Extensions of Gaussian—Type Basis Sets for Use in Molecular Orbital Studies of Organic Molecules. *J. Chem. Phys.* **1972,** *56*, 2257-2261.

52. Marenich, A. V.; Cramer, C. J.; Truhlar, D. G. Universal Solvation Model Based on Solute Electron Density and on a Continuum Model of the Solvent Defined by the Bulk Dielectric Constant and Atomic Surface Tensions. *J. Phys. Chem. B* **2009,** *113*, 6378-6396.

53. Todd A. Keith, T. G. S., Overland Park KS, USA, 2019 (aim.tkgristmill.com) *AIMAll (Version 19.10.12)*.

Table of Contents Graphics: